Local fluxes in MHD Turbulence

Alexandros Alexakis [1]†& Sergio Chibbaro [2]

Laboratoire de Physique de lEcole Normale Suprieure, ENS, Universit PSL, CNRS, Sorbonne Universit, Universit Paris-Diderot, Sorbonne Paris Cit, Paris, France,

[2]Université Paris-Saclay, CNRS, LISN, 91400 Orsay, France

(Received xx; revised xx; accepted xx)

Using highly resolved direct numerical simulations we examine the statistical properties of the local energy flux rate $\Pi_\ell(x)$ towards small scales for three isotropic turbulent magnetohydrodynamic flows, which differ in strength and structure of the magnetic field. We analyse the cascade process both in the kinetic and magnetic energy, disentangling the different flux contributions to the overall energy dynamics. The results show that the probability distribution of the local energy flux develops long tails related to extreme events, similar to the hydrodynamic case. The different terms of the energy flux display different properties and show sensitivity on the type of the flow examined. We further examine the joint pdf between the local energy flux and the gradients of the involved fields. The results point out a correlation with the magnetic field gradients, showing however a dispersion much stronger than what is observed in hydrodynamic flows. Finally, it is also shown that the local energy flux shows some dependence on the local amplitude of the magnetic field. The present results have implications for subgrid scale models that we discuss.

1. Introduction

Most stellar objects from stars to galaxies are made of hot gas in a ionized state. The magneto-hydrodynamic (MHD) equations give the simplest description of the dynamics involved (Goldstein *et al.* 1995; Battaner 1996; Biskamp 2003; Verma 2004; McKee & Ostriker 2007; Bruno & Carbone 2013; Galtier 2016) and give a general framework relevant for dynamo and many plasma phenomena (Landau *et al.* 2013; Brandenburg & Subramanian 2005; Davidson 2002). At large Reynolds numbers (small dissipation parameters) the MHD turbulent dynamics become turbulent sharing many features with hydrodynamic turbulence. The key idea is the existence of *cascade* processes, meaning that inviscid invariants are transferred across scales so that they are efficiently dissipated at the smallest scales (Monin & Yaglom 1975; Frisch 1995; Alexakis & Biferale 2018). This idea sketched by Richardson, was at the basis of the phenomenological statistical theory by Kolmogorov (Kolmogorov 1941; Kraichnan 1971) and is the cornerstone of our understanding of turbulence. Different theories have been proposed that attempt to describe quantitatively the behavior of MHD turbulence (Iroshnikov 1964; Kraichnan 1965). Yet, MHD turbulence displays an even more complex behaviour than Hydrodynamic one with diverse regimes and recently new theories have been proposed (Goldreich & Sridhar 1995; Boldyrev 2006; Beresnyak 2011). A variety of methods have been applied in MHD to test and constrain existing theories. Two point correlation functions have led to some constraints on third order structure functions (Politano & Pouquet 1998; Galtier 2009). Scale by scale analysis in Fourier space that has been extensively used in hydrodynamics (Chen *et al.* 2003; Domaradzki *et al.* 2009; Teaca *et al.* 2011; Alexakis *et al.* 2007; Verma

† Email address for correspondence: alexakis@phys.ens.fr

2004, 2019) has been applied with some success in MHD as well (Verma 2021; Dar *et al.* 2001; Teaca *et al.* 2009; Alexakis *et al.* 2005; Mininni *et al.* 2005).

New insights on the cascade physics have been obtained analysing the scale-by-scale budgets of energy of filtered fields, including the fluctuations of the flux (Eyink & Sreenivasan 2006; Dubrulle 2019). Notably, this kind of complex tools have been used to get insights on the physical mechanisms in 2D and 3D fluid turbulence (Piomelli *et al.* 1991; Eyink & Aluie 2009; Eyink 2005; Liu *et al.* 1994; Chen *et al.* 2006) and more recently, scale-by-scale filtering analysis has been started to be applied also to MHD turbulence to highlight and understand some specific processes (Eyink *et al.* 2013; Galtier 2018; Bian & Aluie 2019). The interest of such tools is witnessed by its use in many other problems such as two-fluid plasma models (Camporeale *et al.* 2018), hybrid-kinetic models (Cerri & Camporeale 2020), gyro-kinetics (Teaca *et al.* 2021), and full-kinetic systems (Eyink 2018; Yang *et al.* 2022). More generally, this kind of approach seems promising to go beyond standard statistical information and access to energetic processes, which are usually the most important for applications, and are nowadays commonly used in a variety of cases (Danaila *et al.* 2001; Casciola *et al.* 2003; Sorriso-Valvo *et al.* 2007; Cimarelli *et al.* 2013; Valori *et al.* 2020; Innocenti *et al.* 2021). Our work follows this path in order to get similar understanding for MHD turbulence.

Such an understanding of the cascade process is paramount for astrophysical and industrial applications for the following reason. While the numerical solution of the fundamental equations is in principle possible, the vast range of scales excited in such objects prohibits any direct numerical calculation that resolves all the scales down to the dissipation ones. However, if all scales are not properly resolved, the numerical approach is tantamount to apply a coarse-graining to the initial problem discarding a part of the information, related to the small scales not resolved. As a result all simulations of astrophysical flows require some modeling of smaller unresolved scales that are responsible for the energy dissipation. Such modeling will thus have to compensate the energy transfers between resolved and unresolved scales so that it correctly captures the energy dissipation of the flow. The construction of such models requires a deep and quantitative understanding of how turbulence transfers energy to small scales.

This practice to compute only large scales and to put forward approximate models at small scales is referred to as Large-eddy simulations (LES), and has a long history in fluid turbulence in particular for practical applications (Leonard 1975; Germano 1992; Meneveau & Katz 2000; Sagaut 2001; Lesieur *et al.* 2005; Pope 2000). In hydrodynamic turbulence the development and testing of such models is thus well advanced. A particular class of hydrodynamic models quantify the dissipation energy by a an eddy-viscosity term whose coefficient depends on the gradients of the resolved flow (Smagorinsky 1963; Germano *et al.* 1991; Germano 1992), and many studies have been devoted in quantifying this dependence (Vreman *et al.* 1994, 1997; Borue & Orszag 1998; Meneveau & Katz 2000).

In MHD, LES is less developed and tested than in fluid turbulence. At the same time the complexity of the MHD is increased as more channels exist for the energy to be transferred to the smaller scales and since there are two fields involved there are more possibilities for the dependence of the eddy viscosity term. A convenient way to assess subgrid models is through direct numerical simulations, which are however more difficult than in hydrodynamics and only recently DNS with a sufficient resolution allowing for an inertial range to be present have been made available. Yet, Smagorinski-like models have been adapted through formal analogy in MHD since the 90' (Theobald *et al.* 1994; Müller & Carati 2002; Verma & Kumar 2004; Bian *et al.* 2021). These models still represent the only available strategy for subgrid modelling (Miesch *et al.* 2015), and they have been

recently generalised even to compressible (Chernyshov *et al.* 2014; Vlaykov *et al.* 2016; Grete *et al.* 2017) and relativistic MHD (Viganò *et al.* 2019; Carrasco *et al.* 2020).

Although DNS has been used to partially assess the validity of such closures (Agullo *et al.* 2001; Miesch *et al.* 2015; Kessar *et al.* 2016), a thorough analysis is still needed, given the importance of the problem. Notably, in the last years, new analysis of this kind of modelling has been made possible by the use of scale-by-scale analysis (Linkmann *et al.* 2018; Biferale *et al.* 2019; Buzzicotti *et al.* 2018; Alexakis & Chibbaro 2020). In these works, it has been pointed out that a deeper understanding of the cascade process, including fluctuations is valuable also to improve modelling.

The purpose of this work is to shed some light on this direction by examining different MHD turbulence flows and the statistical properties of the local energy flux towards the smaller scales, bringing to MHD this original approach already applied to hydrodynamic turbulence. In particular, we analyse the scale-by-scale budgets of kinetic and magnetic energy of highly resolved DNS. That allows to provide new information on the cascade process, including fluctuations, and thus to go beyond usual investigation about the validity of subgrid models. As a final introductory comment, it is worth emphasising that our goal is not to put forward and/or test some specific model but rather to get some insights on the modelling via DNS.

2. Theoretical formulation

2.1. *Main Equations*

We begin by considering the magneto-hydrodynamic equations in the incompressible non-relativistic limit, given by (Biskamp 2003)

$$\frac{\partial \mathbf{u}}{\partial t} + \mathbf{u}\cdot\nabla\mathbf{u} = -\nabla p + \mathbf{b}\cdot\nabla\mathbf{b} + \nu\nabla^2\mathbf{u} \tag{2.1}$$

$$\frac{\partial \mathbf{b}}{\partial t} + \mathbf{u}\cdot\nabla\mathbf{b} = \mathbf{b}\cdot\nabla\mathbf{u} + \eta\nabla^2\mathbf{b}, \tag{2.2}$$

$$\nabla\cdot\mathbf{v} = 0, \quad \nabla\cdot\mathbf{b} = 0, \tag{2.3}$$

where the modified pressure p is given by $p = P/\rho + b^2/2$, $\mathbf{b} = \mathbf{B}\sqrt{4\pi\rho}$, and ρ is the mass density, $\mathbf{u}(\mathbf{x},t)$ is the flow velocity, $P(\mathbf{x},t)$ is the thermal pressure, $\mathbf{B}(\mathbf{x},t)$ is the magnetic induction field ν is the viscosity and η the magnetic diffusivity.

2.2. *Scale-By-scale Analysis*

A considerable amount of work in analysing the transfer of energy among scales has been performed in Fourier space with significant results (Domaradzki *et al.* 2009; Alexakis *et al.* 2007; Teaca *et al.* 2011; Verma 2004, 2019, 2021; Teaca *et al.* 2009; Alexakis *et al.* 2005; Mininni *et al.* 2005). This kind of approach while useful in understanding and quantifying the scale-by-scale energy budget of turbulence, does not allow to simply link the related energy transfers with local properties of the flow and thus limits their applicability to subgrid scale models.

To analyse the local in space scale-by-scale dynamics, we use the local filtering approach (Germano 1992). We introduce a filter such that

$$\widetilde{\mathbf{a}}_\ell(\mathbf{x}) = \int dr^3\, G_\ell(\mathbf{r})\mathbf{a}(\mathbf{x}+\mathbf{r}) \tag{2.4}$$

where $G(\mathbf{r})$ is a smooth filtering function, spatially localized and such that $\int dr^3\, G(\mathbf{r}) = 1$, and $\int dr^3\ |\mathbf{r}|^2 G(\mathbf{r}) \approx 1$. The function G_ℓ is rescaled with ℓ as $G_\ell(\mathbf{r}) = \ell^{-3}G(\mathbf{r}/\ell)$. Applying this filter to the MHD equations one obtains (Aluie 2017):

$$\partial_t \widetilde{\mathbf{u}}_\ell + (\widetilde{\mathbf{u}}_\ell \cdot \nabla)\widetilde{\mathbf{u}}_\ell = -\nabla \widetilde{p}_\ell + (\widetilde{\mathbf{b}}_\ell \cdot \nabla)\widetilde{\mathbf{b}}_\ell - \nabla \cdot (\boldsymbol{\tau}_\ell^{uu} - \boldsymbol{\tau}_\ell^{bb}) + \nu \nabla^2 \widetilde{\mathbf{u}}_\ell. \tag{2.5}$$

$$\partial_t \widetilde{\mathbf{b}}_\ell + (\widetilde{\mathbf{u}}_\ell \cdot \nabla)\widetilde{\mathbf{b}}_\ell - (\widetilde{\mathbf{b}}_\ell \cdot \nabla)\widetilde{\mathbf{u}}_\ell = -\nabla \cdot (\boldsymbol{\tau}_\ell^{ub} - \boldsymbol{\tau}_\ell^{bu}) + \eta \nabla^2 \widetilde{\mathbf{b}}_\ell \tag{2.6}$$

$$\nabla \cdot \widetilde{\mathbf{b}}_\ell = \nabla \cdot \widetilde{\mathbf{u}}_\ell = 0. \tag{2.7}$$

Here $\boldsymbol{\tau}_\ell^{uu}, \boldsymbol{\tau}_\ell^{bb}, \boldsymbol{\tau}_\ell^{ub}$ and $\boldsymbol{\tau}_\ell^{bu}$, are the *subscale stress tensors* which describe the force exerted on scales larger than ℓ by fluctuations at scales smaller than ℓ. They are defined as

$$\boldsymbol{\tau}_\ell^{uu} = \widetilde{(\mathbf{uu})}_\ell - \widetilde{\mathbf{u}}_\ell \widetilde{\mathbf{u}}_\ell, \qquad \boldsymbol{\tau}_\ell^{bb} = \widetilde{(\mathbf{bb})}_\ell - \widetilde{\mathbf{b}}_\ell \widetilde{\mathbf{b}}_\ell \tag{2.8}$$

are the *subscale Reynolds stress* and the *subscale Maxwell stress* respectively and finally

$$\boldsymbol{\tau}_\ell^{ub} = \widetilde{(\mathbf{ub})}_\ell - \widetilde{\mathbf{u}}_\ell \widetilde{\mathbf{b}}_\ell, \qquad \boldsymbol{\tau}_\ell^{bu} = \widetilde{(\mathbf{bu})}_\ell - \widetilde{\mathbf{b}}_\ell \widetilde{\mathbf{u}}_\ell \tag{2.9}$$

are cross-field tensors for which one is the transpose of the other $\boldsymbol{\tau}_\ell^{bu} = [\boldsymbol{\tau}_\ell^{ub}]^T$.

Using this notation we can write an equation for the large scale energy densities $\tilde{\mathcal{E}}^u = \frac{1}{2}|\widetilde{\mathbf{u}}|^2$ and $\tilde{\mathcal{E}}^b = \frac{1}{2}|\widetilde{\mathbf{b}}|^2$ as

$$\partial_t \tilde{\mathcal{E}}_\ell^u + \nabla \cdot \mathcal{J}^u = -\Pi_\ell^{uu} - \Pi_\ell^{bb} + \mathcal{W}_L - \mathcal{D}_u \tag{2.10}$$

$$\partial_t \tilde{\mathcal{E}}_\ell^b + \nabla \cdot \mathcal{J}^b = -\Pi_\ell^{bu} - \Pi_\ell^{ub} - \mathcal{W}_L - \mathcal{D}_b \tag{2.11}$$

where the currents $\mathcal{J}^u, \mathcal{J}^b$ are given by

$$\mathcal{J}_j^u = \left(\frac{1}{2}|\widetilde{\mathbf{u}}|^2 + \overline{p}\right)\widetilde{u}_j + (\tau_{\ell,ij}^{uu} - \tau_{\ell,ij}^{bb})\widetilde{u}_i - \nu\frac{1}{2}\partial_j|\widetilde{\mathbf{u}}|^2 \tag{2.12}$$

$$\mathcal{J}_j^b = \left(\frac{1}{2}|\widetilde{\mathbf{b}}|^2\right)\widetilde{u}_j + (\tau_{\ell,ij}^{ub} - \tau_{\ell,ij}^{bu})\widetilde{b}_i - (\widetilde{\mathbf{u}} \cdot \widetilde{\mathbf{b}})\widetilde{b}_j - \eta(\widetilde{\mathbf{b}} \times \nabla \times \widetilde{\mathbf{b}}) \tag{2.13}$$

and express the transport of energy in space. The rate of work done on the flow originating from the Lorentz force is given by

$$\mathcal{W}_L = \widetilde{u}_i \widetilde{b}_j \partial_j \widetilde{b}_i. \tag{2.14}$$

This term is responsible for the transfer of kinetic energy to magnetic energy in the large scales. The viscous and Ohmic energy dissipation rates are given by

$$\mathcal{D}_u = \nu(\partial_j \widetilde{u}_i)(\partial_j \widetilde{u}_i) \quad \text{and} \quad \mathcal{D}_b = \eta(\nabla \times \widetilde{\mathbf{b}}) \cdot (\nabla \times \widetilde{\mathbf{b}}) \tag{2.15}$$

and express the rate energy is dissipated by viscous and Ohmic effects respectively. These terms can be shown to be negligible if the filter scale is large and the viscous/resistive coefficients are small (Aluie 2017). Finally the four fluxes in scale space $\Pi_\ell^{uu}, \Pi_\ell^{bb}, \Pi_\ell^{ub}, \Pi_\ell^{bu}$, explicitly given by:

$$\Pi_\ell^{uu} = -\tau_{\ell,ij}^{ub}\partial_i \widetilde{u}_j = -[\widetilde{(u_i u_j)}_\ell - \tilde{u}_{\ell,i}\tilde{u}_{\ell,j}]\partial_i \widetilde{u}_j \tag{2.16}$$

$$\Pi_\ell^{bb} = +\tau_{\ell,ij}^{bb}\partial_i \widetilde{u}_j = +[\widetilde{(b_i b_j)}_\ell - \tilde{b}_{\ell,i}\tilde{b}_{\ell,j}]\partial_i \widetilde{u}_j \tag{2.17}$$

$$\Pi_\ell^{ub} = -\tau_{\ell,ij}^{ub}\partial_i \widetilde{b}_j = -[\widetilde{(u_i b_j)}_\ell - \tilde{u}_{\ell,i}\tilde{b}_{\ell,j}]\partial_i \widetilde{b}_j \tag{2.18}$$

$$\Pi_\ell^{bu} = +\tau_{\ell,ij}^{bu}\partial_i \widetilde{b}_j = +[\widetilde{(b_i u_j)}_\ell - \tilde{b}_{\ell,i}\tilde{u}_{\ell,j}]\partial_i \widetilde{b}_j \tag{2.19}$$

express the rate of gain (if $\Pi_\ell < 0$) or loss (if $\Pi_\ell > 0$) of energy of the large scales to the

small filtered-out scales. Their sum gives the total energy flux

$$\Pi_\ell(\mathbf{x}) = \Pi_\ell^{uu}(\mathbf{x}) + \Pi_\ell^{bb}(\mathbf{x}) + \Pi_\ell^{ub}(\mathbf{x}) + \Pi_\ell^{bu}(\mathbf{x}) \tag{2.20}$$

The fluxes are chosen so that they are invariant under Galilean transformations $\mathbf{u} \to \mathbf{u} + \mathbf{U}_0$ and also under $\mathbf{b} \to \mathbf{b} + \mathbf{B}_0$ for any flow realization $\mathbf{u}, \mathbf{b}$, where $\mathbf{U_0}, \mathbf{B_0}$ are constant in space vector fields. The importance of Galilean invariance has been noted in the past (Speziale 1985; Aluie & Eyink 2009, 2010). We note however that while the defined fluxes are invariant under $\mathbf{b} \to \mathbf{b} + \mathbf{B}_0$ the MHD equations are not. Therefore, the introduction of a constant $\mathbf{B}_0$ in the dynamics of the MHD equations will alter the statistical behavior of the fields $\mathbf{u}, \mathbf{b}$ and as a result of the fluxes as well.

The fluxes in (2.16)-(2.19) comprise the main object of the present work.

2.3. *Filters*

Although we formulate our filtering procedure in the physical space, since we will be working in periodic domains it is useful to define the filters through their Fourier transforms

$$\hat{G}_q(\mathbf{k}) = \int G_\ell(\mathbf{x}) e^{i\mathbf{k}\cdot\mathbf{x}} d\mathbf{x} \tag{2.21}$$

where $q = 1/\ell$ is the wavenumber corresponding to the filter length ℓ, not to be confused with the Fourier wavenumber k. For the first filter we consider a Gaussian kernel

$$\hat{G}_q(\mathbf{k}) = \exp\left[-\frac{k^2}{2q^2}\right]. \tag{2.22}$$

For an infinite domain this filter corresponds to the Gaussian filter in real space $G_\ell(r) = \exp(-\frac{1}{2}r^2/\ell^2)/(2\pi\ell^2)^{3/2}$. We note that this filtering is not a projection and in general $\widetilde{(\tilde{\mathbf{u}}_\ell)_\ell} \neq \tilde{\mathbf{u}}_\ell$. The second filter we are going to consider is a sharp spectral filter such that

$$\widetilde{\mathbf{u}}_\ell(\mathbf{x}, t) = \sum_{|\mathbf{k}|<q} \hat{\mathbf{u}}(\mathbf{k}, t) e^{i\mathbf{k}\cdot\mathbf{x}}. \tag{2.23}$$

This filtering is a projector $\widetilde{(\widetilde{\mathbf{u}}_\ell)_\ell} = \widetilde{\mathbf{u}}_\ell$ and is based on a Galerkin truncation for all wavenumbers larger than the given cutoff $q = 1/\ell$. With regard to the representation of energy fluxes, this filter has been shown in the past not to be optimal as it leads to a wider fluctuations of the local energy flux (Buzzicotti *et al.* 2018; Alexakis & Chibbaro 2020), something that as we will show also holds in MHD.

3. Sub-scale stress modeling

In this section, we provide some information about typical modelling strategy. Our work focuses on fundamental issues, that allows us to build a precise framework and to point to possible applications.

In a simulation for which only the large smoothed out fields $\widetilde{\mathbf{u}}, \widetilde{\mathbf{b}}$ fields are followed dynamically the effect of the small unresolved scales on the resolved scales need to be captured by modeling the sub-scale stress tensors $\boldsymbol{\tau}_\ell^{uu}, \boldsymbol{\tau}_\ell^{ub}, \boldsymbol{\tau}_\ell^{bu}, \boldsymbol{\tau}_\ell^{bb}$. In hydrodynamics, the simplest perhaps such model is formed by assuming that $\boldsymbol{\tau}^{uu}$ takes the form

$$\boldsymbol{\tau}_{\ell,ij}^{uu} = \nu_{\ell,ijkl}^e \nabla_k \widetilde{\mathbf{u}}_l \tag{3.1}$$

where the eddy viscosity tensor ν^e is a function of space and time and needs to be prescribed from the filtered field $\widetilde{\mathbf{u}}$ in order for the filtered equations to be closed. It needs to satisfy $\langle \nabla_i \widetilde{\mathbf{u}}_j \nu_{\ell,ijkl}^e \nabla_k \widetilde{\mathbf{u}}_l \rangle = \epsilon > 0$ and acts thus on average as a sink of

energy. Furthermore, the divergence of $\nabla \cdot \boldsymbol{\tau}_\ell^{uu}$ is not necessarily zero so its projection to divergence free vector fields needs to be considered by adding $p' = \nabla^{-2}\nabla_i\nabla_j\tau^{uu}_{\ell,ij}$ to the pressure. Since the system is Galilean invariant ν^e cannot depend on the values of $\widetilde{\mathbf{u}}$ but only on its gradients $\nabla\widetilde{\mathbf{u}}, \nabla\nabla\widetilde{\mathbf{u}}, \ldots$, thus in the simplest case ν^e_ℓ is just a function of $\nabla\widetilde{\mathbf{u}}$. If we further assume that isotropy is present at the small scales $\nu^e[\nabla\widetilde{\mathbf{u}}]$ will only depend on the invariants (under rotations and reflections) of the strain tensor $\nabla\widetilde{\mathbf{u}}$. In the now classical Smagorinsky approach the sub-scale Reynolds stress tensor is modeled as (Smagorinsky 1963)

$$\boldsymbol{\tau}^{uu}_{\ell,ij} - \frac{1}{3}\boldsymbol{\tau}^{uu}_{\ell,kk} = \nu^e_\ell \widetilde{S}_{ij} = \frac{\nu^e}{2}\left(\partial_i\tilde{u}_j + \partial_j\tilde{u}_i\right) \tag{3.2}$$

where $\widetilde{\mathbf{S}}$ is the symmetric part of the filtered strain tensor. The ν^e is a scalar defined as (Smagorinsky 1963)

$$\nu^e_\ell = c\ell^2|\widetilde{\mathbf{S}}| = c\ell^2\sqrt{\tilde{S}_{ij}\tilde{S}_{ij}} \tag{3.3}$$

where ℓ is the filtering lengthscale and c is the Smagorinsky constant, an order one non-dimensional coefficient . Eq. (3.3) gives the only combination of ℓ and $|\widetilde{\mathbf{S}}|$ with dimensions of viscosity. We note that in general ν^e_ℓ depends on space and needs to be taken in to account for the pressure so that the divergence free condition for $\widetilde{\mathbf{u}}$ is satisfied.

This model implies that the flux of energy to the small scales is given by

$$\Pi_\ell(\mathbf{x}) = c\ell^2|\widetilde{\mathbf{S}}|^3. \tag{3.4}$$

After Smagorinsky's work other models that also take into account the anti-symmetric part of the stress tensor

$$\widetilde{\Omega}_{ij} = \frac{1}{2}\left(\partial_i\tilde{u}_j - \partial_j\tilde{u}_i\right) \tag{3.5}$$

have been developed. Approximating the sub-scale stress with its extreme local expression, the nonlinear Clark model is obtained (Meneveau & Katz 2000):

$$\tau^{uu}_\ell \approx \frac{1}{3}C_2\ell^2\left(\widetilde{\mathbf{S}}^2_\ell + \widetilde{\Omega}^2_\ell + \widetilde{\Omega}_\ell\widetilde{\mathbf{S}}_\ell - \widetilde{\mathbf{S}}_\ell\widetilde{\Omega}_\ell\right) , \tag{3.6}$$

where both strain and vorticity participate in the dynamics (Misra & Pullin 1997; Borue & Orszag 1998; Tennekes & Lumley 1990) and leads to modeled local energy flux:

$$\Pi_\ell \approx \frac{1}{3}C_2\ell^2[-\mathrm{Tr}(\widetilde{\mathbf{S}}^3_\ell) + 3\mathrm{Tr}(\widetilde{\mathbf{S}}_\ell\widetilde{\Omega}^2_\ell)] . \tag{3.7}$$

The development and assessment of such models has been often guided by *a priori* analysis (Piomelli *et al.* 1991; Meneveau 1994; Borue & Orszag 1998; Meneveau & Katz 2000), that is studying the filtered DNS field properties rather than resorting to actual LES. Following this approach, in Alexakis & Chibbaro (2020) we have demonstrated that there is indeed a strong correlation between Π_ℓ and $|\widetilde{\mathbf{S}}|$ verifying the Smagorinsky relation (3.4) for the mean value of Π_ℓ although strong fluctuations in Π_ℓ were also measured making Π_ℓ not a strictly positive quantity.

In MHD a similar type of modeling is considerably more difficult. First of all there are three sub-scale turbulent stresses that need to be modeled $\boldsymbol{\tau}^{uu}_\ell, \boldsymbol{\tau}^{ub}_\ell, \boldsymbol{\tau}^{bb}_\ell$. In the past literature these dependencies are modeled based on the symmetric and anti-symmetric parts of the stress tensors of the two fields:

$$\widetilde{S}_{ul,ij} = \frac{1}{2}\left(\partial_i\widetilde{u}_j + \partial_j\widetilde{u}_i\right), \quad \widetilde{\Omega}_{ul,ij} = \frac{1}{2}\left(\partial_i\widetilde{u}_j - \partial_j\widetilde{u}_i\right), \tag{3.8}$$

$$\widetilde{S}_{bl,ij} = \frac{1}{2}\left(\partial_i \widetilde{b}_j + \partial_j \widetilde{b}_i\right), \quad \widetilde{\Omega}_{bl,ij} = \frac{1}{2}\left(\partial_i \widetilde{b}_j - \partial_j \widetilde{b}_i\right). \tag{3.9}$$

An in depth discussion of different models used can be found in Müller & Carati (2002); Miesch *et al.* (2015). Furthermore, although the system is still Galilean invariant, it is not invariant under transformation $\mathbf{b} \to \mathbf{b} + \mathbf{B_0}$ where $\mathbf{B_0}$ is a constant in space magnetic field. The statistics of the sub-filter scale fields can depend on the local value of $\widetilde{\mathbf{b}}$ and as a result so will the relevant eddie-viscosities that attempt to model their effect. Finally, in the presence of helicity the small scales are known to transfer energy to the large scales in a mean way by the alpha dynamo mechanism that modeling needs to take into account.

Given the large number of the properties of the smoothed fields that the modeling of the sub-scale turbulent stresses can depend on, it is important to try to limit the possibilities identifying the parameters that play the most important role. This is what we are attempting to do in the following sections using direct numerical simulations for which the turbulent stresses can be directly measured. Thus, we need to stress that we do not test a posteriori any proposed model. Instead we are trying a priori to find relations that hold between the local energy flux and the gradients of the flow so that they can be used in the construction of new models.

4. Numerical Simulations

4.1. *Numerical Set-up*

To investigate the local energy fluxes described before we use the results from direct numerical simulations DNS using the pseudo-spectral code GHOST (Mininni *et al.* 2011) evolving the MHD equations (2.1)-(2.3) in a cubic triple periodic domain of side $L = 2\pi$ so that $|\mathbf{k}| = \mathbf{1}$ give the smallest non-zero wavenumber . The forcing is limited only to wave numbers with $|\mathbf{k}| \leqslant k_f = 2$ in all cases and was random and delta correlated in time so that the mean energy injection rate $\epsilon = \langle \mathbf{u} \cdot \mathbf{f_u} \rangle + \langle \mathbf{b} \cdot \mathbf{f_b} \rangle = 1$ is independent of the flow state. All runs have the same energy injection rate and unit Prandtl number with $\nu = \mu = 0.0001$. The involved Reynolds number based on the input parameters ϵ, L and ν is given by $Re = \epsilon^{1/3} k_f^{4/3}/\nu$ that is thus fixed to $Re = 3968$. The resolution was fixed for all runs at $N = 1024$ grid points in each direction that was sufficient for the flow to be well resolved so that an exponential decrease of the energy spectrum is observed at large k. No artificial dissipation was used.

Four different cases were considered. In the first, no magnetic forcing was introduced and the magnetic field was set identically to zero $\mathbf{b} = \mathbf{0}$ so that the flow reduced to a hydrodynamic run, repeating essentially the results of Alexakis & Chibbaro (2020). This run is used as a reference to identify the differences of MHD from hydrodynamic runs and referred in the subsequent figures as 'Hydro'. The remaining three runs were designed to have different levels of magnetic energy as in Alexakis (2013). The second run was thus a dynamo run. No magnetic forcing was used but an initial small magnetic field was introduced that was amplified by the turbulent motions until a steady state was reached where the magnetic energy fluctuated around a mean value. We note that the forcing was mirror symmetric so no helicity is injected in the system. A result of the absence of helicity and the randomness of the flow is that magnetic energy is concentrated in the small scales. This run is referred to in the figures as 'dynamo'. In the third run a magnetic forcing was also used of equal magnitude as the mechanical flow. The resulting flow at steady state has magnetic energy at equipartition with the kinetic energy at all scales. The helicity and magnetic helicity injection rate for this flow is also set to zero. Results from this run are referred to as 'moderate'. Finally the fourth flow has also both

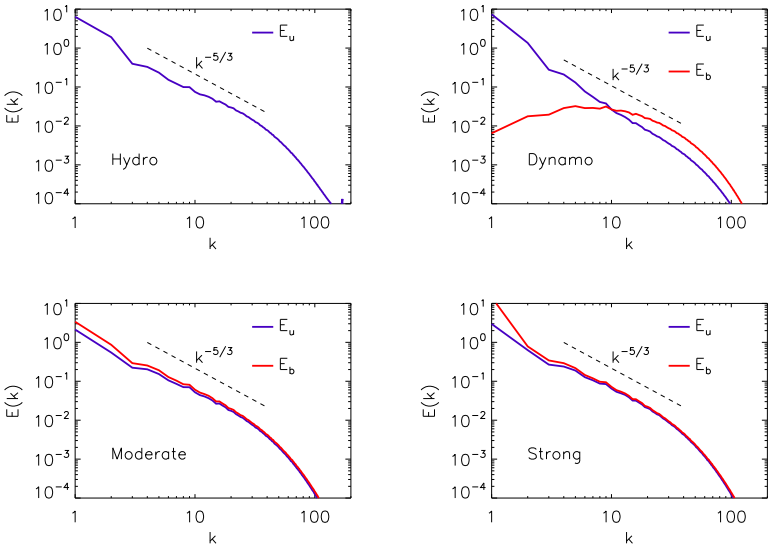

Figure 1: Energy Spectra for the 4 different cases examined.

mechanically and magnetically forced but in this case the magnetic helicity was weak but not zero. This has lead to the formation of a slowly growing large scale helical magnetic field. As a result this flow has magnetic energy that exceeds the kinetic energy of the flow. This run is referred to in the figures as 'strong'.

It is worth noting that all the statistics we present in the following are obtained through time-averaging over a large amount of samples during the steady state to assure statistical convergence. Whenever possible, several field realizations have been used also to average over space, thanks to spatial homogeneity.

4.2. *Energy Spectra and Magnetic field*

Figure 1 shows the resulting time-averaged energy spectra for the four runs at the steady state. For the dynamo run in particular analysis is made at the state such that magnetic energy does not grow anymore. All runs show energy spectra compatible with a $k^{-5/3}$ power-law exponent. The magnetically forced runs 'moderate' and 'strong' have equipartition magnetic energy across wave numbers except for $k = 1$ in the 'strong' case for which magnetic energy is larger. For the dynamo run the magnetic energy is weaker than kinetic at small wave numbers but the reverse is true for the large wavenumbers. This behavior is typical for randomly forced non-helical small scale dynamos (Schekochihin *et al.* 2004; Moll *et al.* 2011; Brandenburg *et al.* 2012). Dynamo flows with steady non-helical forcing, like Taylor-Green for example (Ponty *et al.* 2008), produce spectra closer to the 'moderate' run. This figure points out also that a quasi-inertial range is roughly displayed over about a decade between $k = 4$ and $k = 64$, as standard with present resolution.

In figure 2, it is possible to get some qualitative insights on the different cases studied. Notably, the visualization of the magnetic energy permits to observe the structure of the large scales, through its space distribution. The dynamo case displays very little dispersion of the magnetic field amplitude, and energy is concentrated in flux tubes. The moderate case shows a larger distribution and some regions of intense field. Finally the

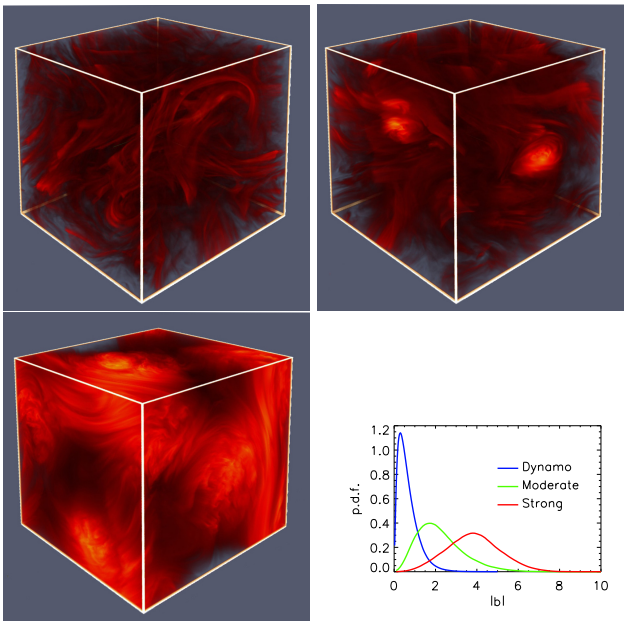

Figure 2: Top panels: Visualisations of the magnetic energy density for the dynamo (top left) the moderate case (top right) and the strong case (bottom left). The bottom panel shows the PDF of $|\mathbf{b}|$ for the 3 different MHD flows examined.

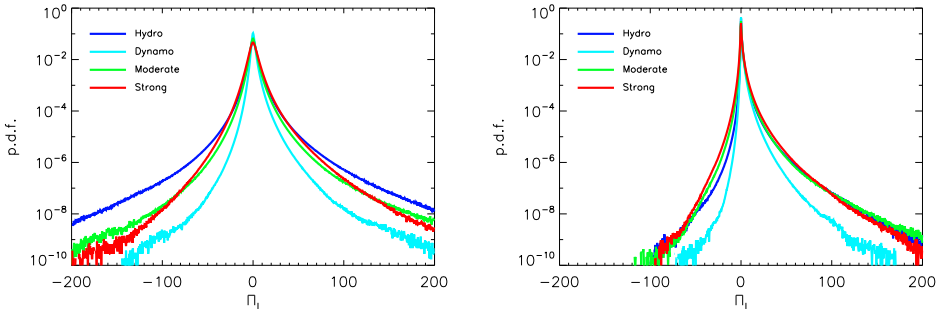

Figure 3: Pdf of the total nonlinear flux $\Pi_\ell(x)$ at $q = 32$ for a sharp spectral filter on the left and a Gauss filter on the right, for the 4 different runs.

strong case shows a much more widely distributed energy, with some regions characterised by large values of the magnetic field, and in particular large-scale structures are visible. To give a quantitative picture, we also show in figure 2 the probability distribution of the magnetic amplitude $|\mathbf{b}|$ for the three MHD cases examined. In the dynamo case the maximum is at small $|\mathbf{b}|$, with a peaked distribution. The width of the distribution increases in the other two cases, with a broad distribution for the strong case. In this last case, the tails appear substantial.

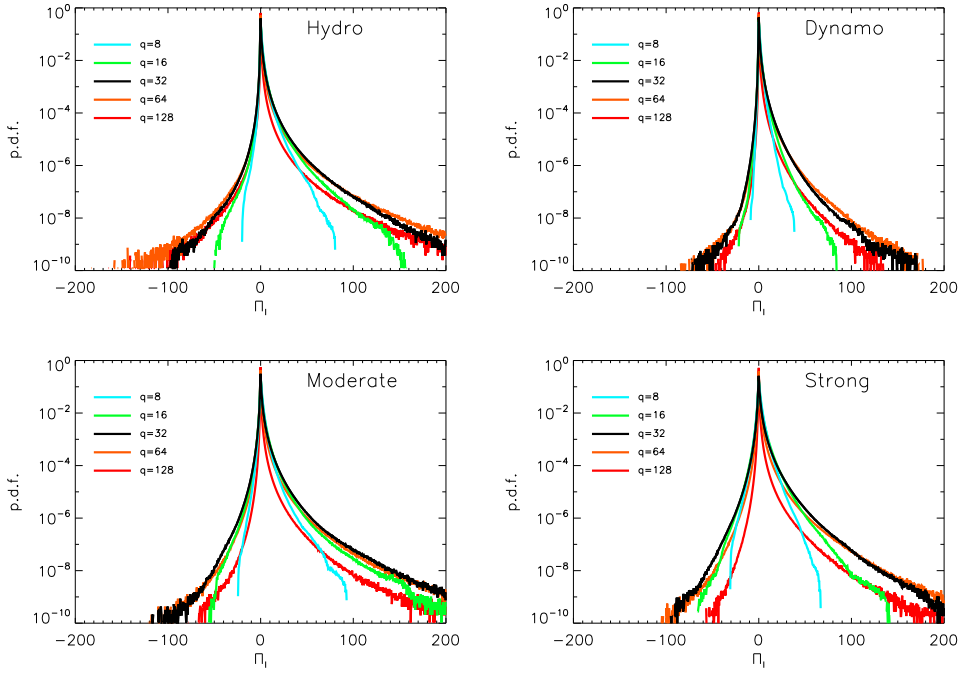

Figure 4: Pdf of the Energy flux for different q for the three MHD cases. In the first panel, the hydro case is also plotted for comparison.

5. Statistics of the local energy flux

The local energy fluxes $\Pi_\ell^{uu}(x)$, $\Pi_\ell^{ub}(x)$, $\Pi_\ell^{bu}(x)$, $\Pi_\ell^{bb}(x)$ and $\Pi_\ell(x)$ were calculated for the four different runs at their steady state. Figure 3 shows this pdf for the four different runs using a sharp-spectral filter (left) and Gaussian filter (right) for a filter length $q = 32$, which corresponds to a value at around the end of the inertial range.

As in hydrodynamics, in MHD the sharp-spectral filter leads to a wider and more symmetric pdf of Π_ℓ. Interestingly, the pure hydro curve presents the strongest tails, while with the Gaussian filter the profiles were found always similar. Considering the representation of the fluxes, the sharp-filter is thus found to enhance fluctuations displaying many negative events, making it more difficult to use directly in LES. The reason for this behavior is the fact that the sharp filter is not localised in space and not positive-definite. For this reason, it appears less useful for the analysis of the energy fluxes and it is abandoned in the following. In this sense, the present analysis confirms previous results obtained in the pure hydrodynamic case (Buzzicotti *et al.* 2018; Alexakis & Chibbaro 2020).

The Gaussian filter leads for all four cases to a skewed pdf with non-Gaussian (stretched exponential) tails. The tails for all cases extend to values hundred times more than the mean value $\langle \Pi_\ell \rangle = 1$, implying that, although rare, these events can play a significant role in the dynamics. The most notable result when comparing the four different cases is that the dynamo run has weaker tails than the other flows. It turns out hence that the dynamo dynamics suppresses efficiently extreme energy flux fluctuations. Small differences are experienced between the moderate and strong cases, indicating that fluid fluctuations are not affected by the large helical magnetic field, which is present only in the strong

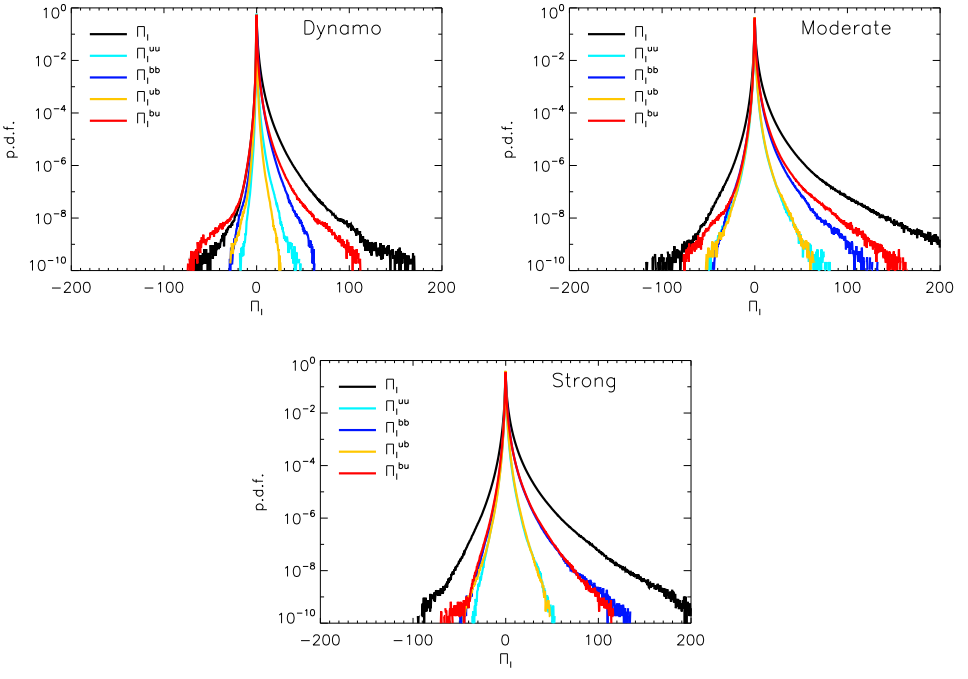

Figure 5: The Different components of the Energy flux for $q = 32$. The total flux is also plotted for information. The three MHD cases are considered.

case. It is possible to observe just a slight increase in the probability of negative events with respect to positive ones. Still, not much difference is found neither comparing the moderate/strong cases to the hydro case.

The statistical behaviour of the energy flux Π_ℓ is further studied in Figure 4. Here we present the probability density function of the flux Π_ℓ at different scales $\ell = 1/q$, for the 4 different cases. The hydro results are given for comparison. The first remark is that as said above, the dynamo case is quite different from the others, with more shrunk distributions, though the distribution remains tailed and skewed. All the cases displays similar changes with going towards smaller scales. The profiles are much less wide in the large-scale range $q = 8, 16$, notably for $q = 8$. Then, the distributions are basically indistinguishable for $q = 32, 64$, which are more or less in the far inertial range, and finally the tails are again reduced for $q = 128$, which is in the dissipation range. As expected, intermittency is maximum at the end of the inertial range. Slight differences between the moderate and the strong case can be detected, yet not significant.

Now, we turn our attention to the four different components of the total energy flux $\Pi_\ell(x)$. In Figure 5. We compare all the terms $\Pi_\ell^{uu}(x)$, $\Pi_\ell^{ub}(x)$, $\Pi_\ell^{bu}(x)$, $\Pi_\ell^{bb}(x)$ composing Π_ℓ as given by Eqs. (2.16)-(2.19). The fluxes show different behavior in the three different cases examined.

The first striking observation is that in all cases the pure hydrodynamic flux, is the smallest one. Most notably, it shows the least important negative fluctuations. It was not possible to infer that from looking only at the total flux Π_ℓ, which is found in Fig. 2 to be similar in the hydro and all the MHD cases. In the moderate and strong cases, the hydrodynamic flux Π_ℓ^{uu} is basically the same as the cross magnetic-hydro flux Π_ℓ^{ub}, while the two are different for the dynamo case. As a consequence, in all cases the terms found

to be dominant are Π_ℓ^{bu} and Π_ℓ^{bb}, that is the blue and red lines. Therefore, the coupling magnetic term contributing to the kinetic energy flux dominates the pure hydro term. Since the total flux in the hydro case is much similar, except for the dynamo case, it appears that the cascade readjusts to distribute much of the flux in this term, although the total kinetic flux remains unchanged. It is interesting to remark also that in the strong case, where both the velocity and the magnetic fields are fully developed, there is a nice symmetry between the two fluxes, with $\Pi_\ell^{uu} \approx \Pi_\ell^{ub}$, and $\Pi_\ell^{bu} \approx \Pi_\ell^{bb}$. That points out to two very similar cascade processes and could be related to the equipartition of the magnetic and kinetic energy cascade recently conjectured in Bian & Aluie (2019). While for the moderate case this symmetry appears also holding apart from the extreme events, the dynamo case breaks it underlying different physics of the cascade process.

Finally, it is useful to note that all the terms, and hence the total flux, are production terms, that is the flux is in average positive towards smaller scales, even though there may be a significant local negative flux. We note also that in the dynamo case there is a mean transfer of kinetic energy to magnetic energy both by the Π_ℓ^{bb} flux and the $\mathcal{W}_L$ term in the large scales (that we do not examine here). This may alter the transfer balance between the different cases. Concerning the negative fluxes, it is important to remark that, unlike the positive tails, the negative parts of the pdfs are basically the same for all components. This is most notably true for the strong case, but also in the other two cases the differences are limited to the region of extremely rare events, where statistical errors may be substantial. That shows that a change in large scale amplitude of the magnetic field can affect the smaller scale forward cascade process.

6. Joint pdfs

6.1. *Field Gradients*

In order to help the construction of subgrid scale models that are based on the gradients of the resolved fields we need to reveal what correlation exists between the gradients and the local energy flux. In figure 6 we present the joint pdf between Π_ℓ and the modulus squared of the symmetric and anti-symmetric stress tensors $\Omega_{u,\ell}^2, \Omega_{b,\ell}^2, S_{u,\ell}^2, S_{b,\ell}^2$ The results are for a given wavenumber in the inertial range $q = 32$.

The results obtained for the pure hydrodynamic configuration are shown for comparison in the top panel. In this case, the energy flux is essentially uncorrelated with the anti-symmetric part of the strain Ω_ℓ with high probability events for a given Ω_ℓ are concentrated around $\Pi_\ell = 0$. On the other hand, a visible correlation is observed with the modulus of the symmetric part of the strain tensor S_ℓ, with high probability events for a given S_ℓ concentrated around a non zero value of Π_ℓ that increases with S_ℓ. The yellow line corresponds to the Smagorinsky scaling of eq. (3.4). The flux Π_ℓ is concentrated around this line giving support to the Smagorinsky model.

Such correlations are less clear for the MHD results. For the dynamo case in the $\Pi_\ell - \Omega_{u\ell}$ diagram high-probability events are concentrated around $\Pi_\ell = 0$ again. For the $\Pi_\ell - S_{u\ell}$ diagram a much weaker correlation is observed compared to the hydro case. The probability density shows long tails with large Π_ℓ for small $S_{u\ell}$ indicating that $S_{u\ell}$ is not dominant in driving the cascade. A stronger correlation is observed with $\Omega_{b,\ell}^2$ and $S_{b,\ell}^2$. High probability events are aligned with the Smagorinsky scaling (yellow dashed line) but the spread is much higher than in the hydro case. The fact that the correlation with $\Omega_{b,\ell}^2$ and $S_{b,\ell}^2$ look very similar indicates that neither of the two alone is an optimal proxy to estimate the energy flux to the small scales.

The lack of correlation of Π_ℓ with the velocity gradients is even more clear for the

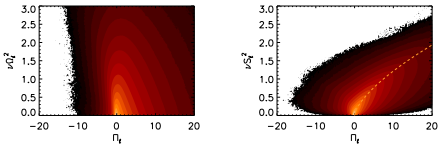

(a) Hydro q=32

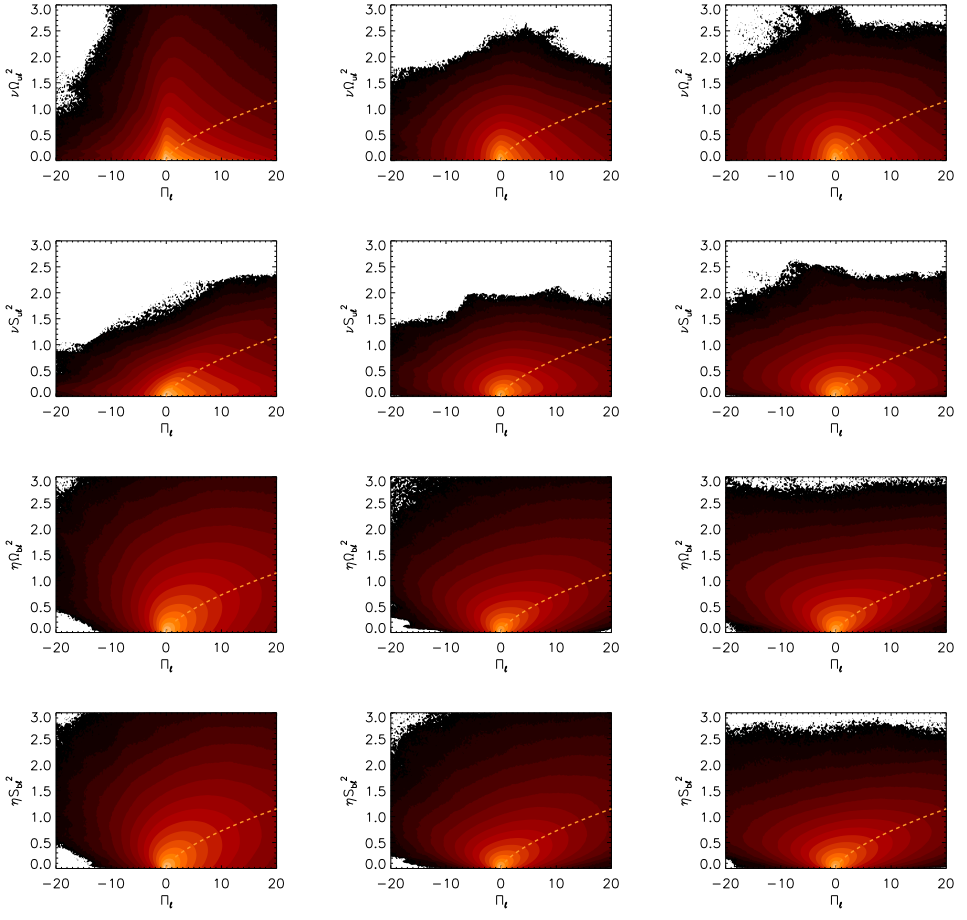

(b) Dynamo q=32 (c) Moderate q=32 (d) Strong q=32

Figure 6: Joint pdfs of Π_ℓ (for $q = 32$) with the modulus of the different strain rates for (a) hydrodynamic case (b) dynamo case (c) moderate case and (d) strong case. From left to right the examined strain is $\Omega^2_{u,\ell}, S^2_{u,\ell}, \Omega^2_{b,\ell}, S^2_{b,\ell}$. Bright colors indicate high probability. The yellow dashed line indicates the Smagorinsky scaling $\Pi_\ell \propto \Omega^{3/2}_\ell$ and $\Pi_\ell \propto S^{3/2}_\ell$.

moderate and strong case. For these cases no correlation is seen neither with $\Omega^2_{u,\ell}$ nor with $S^2_{u,\ell}$. Although there is some correlation with the magnetic field gradients $\Omega^2_{b,\ell}$ and $S^2_{b,\ell}$ with the maximum of probability (for fixed $\Omega^2_{b,\ell}$ or $S^2_{b,\ell}$) following the Smagorinsky scaling (yellow dashed line), the spread is very large with highly probable negative flux events that become more frequent for the strong field case. This indicates that although

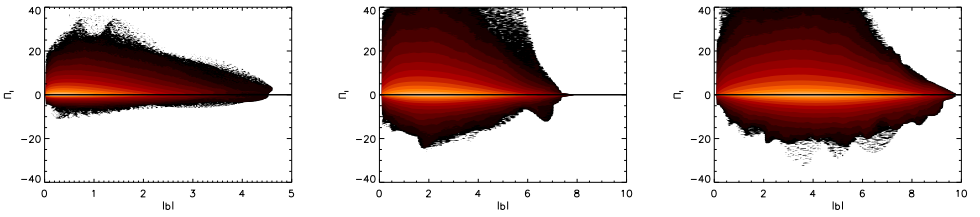

Figure 7: Joint pdf of the local flux Π and the local amplitude of the magnetic field b for the three cases; dynamo (left), moderate (center) and strong (right).

there is some correlation with the magnetic field gradients, modeling the subscale stresses with $\Omega^2_{b,\ell}$ and $S^2_{b,\ell}$ alone is still missing important ingredients.

6.2. *Local magnetic field*

We pursue the analysis of the statistical phenomenology of the cascade process looking at correlations between the flux and the magnetic field. Figure 7 shows the joint PDF of Π_ℓ and $\widetilde{\mathbf{b}}$ for the different cases examined. The three cases display different distributions, with yet similar characteristics. Generally speaking, maximum probability of the flux as well as most extreme values of it are obtained in the region around the average value of the magnetic field. Furthermore, the larger the average magnetic field, the wider the distribution. In this concern, it is interesting to note that the isolines are almost flat over a large range, indicating that in such large region the flux distribution, and therefore the cascade process is basically independent of the value of the magnetic field. That is particularly true for the strong case.

More insight is gained by looking at the pdf of the energy flux conditioned on the knowledge of the magnetic field amplitude. This corresponds at looking at "slices" of Figure 7 for fixed values of $\widetilde{\mathbf{b}}$ and allows to have a more clear look at the extreme events. The results are displayed in Fig. 8. Seen this way some differences can be noted between the three different cases. For the Dynamo there is a monotonic increase of the tails of the distribution with respect to increasing the magnetic field. Both negative and positive tails are wider when related to a larger magnetic field amplitude. In this case large values of $\widetilde{\mathbf{b}}$ indicate more extreme events.

In the moderate case, the probability distribution seems to be almost insensitive to changes in the magnetic field amplitude. The distribution would point to an energy cascade somewhat independent of the magnetic field amplitude. Some small differences are actually present in the distributions, but they are not much more important than statistical errors.

For the strong case, the negative tails increase monotonically with the amplitude of the magnetic field. The positive tails, on the other hand are monotonically decreased by increasing the magnetic field. Therefore, in strongly magnetized flows, large $|\mathbf{b}|$ reduces extreme direct cascade fluctuations, while increases inverse cascade fluctuations. In this sense, the skewness of the distribution seems to be affected by the amplitude of the magnetic field. It appears that in regions of very large magnetic field the distribution is made symmetric. Possibly this behavior occurs because locally in regions of large $\widetilde{\mathbf{b}}$ turbulence transitions to a wave turbulence regime that has weaker forward energy flux or by rendering the flow locally quasi-2D. This effect however would require further investigation to be fully understood, and to assess possible finite-size effects.

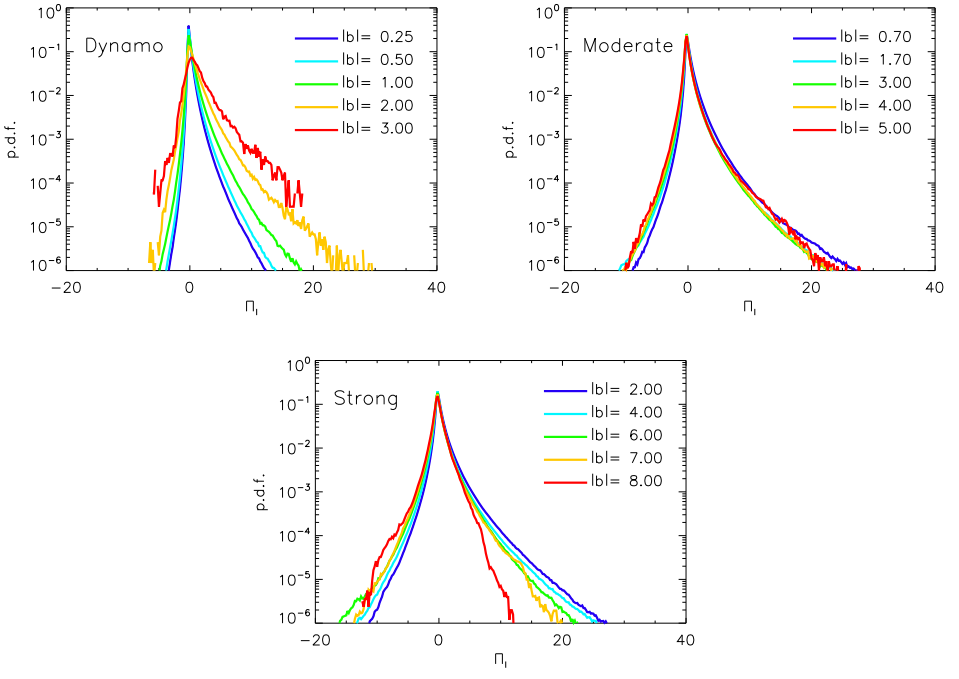

Figure 8: Conditioned pdf *ie* Probability of having flux Π_ℓ given the magnetic field amplitude $|\mathbf{b}|$. In dynamo large $|\mathbf{b}|$ enhances large fluctuations.

7. Conclusions

In this work we have analysed the statistics of the local energy flux for three different magneto-hydrodynamic flows. A scale-by-scale analysis in physical space has been carried out that allows us to access relevant information on the energy cascade process that could help the construction of sub-grid scale models.

First, we have found that a Gaussian filter should be preferred to a spectral one with regard to the representation of the Energy fluxes, a result previously obtained for fluid turbulence. Then, the results of the total energy flux showed some similarities with the hydrodynamic case with Π_ℓ showing a skewed distribution with large tails. However, the dynamo case displays clear differences with respect to the other two cases. This is actually a general feature detected for all observables. On the other hand, moderate and strong cases display overall similar trends and profiles, as exposed by the fluxes computed at different scales.

The analysis of the different components of the energy flux has highlighted that the magnetic field plays a dominant role in the forward cascade. Specifically, the term related to the work made against the sub-scale Reynolds stress is negligible. This is a key information for modelling. The negative part of the flux, that is the back-scatter flux, is instead basically the same for all components. Moreover, the study of the correlation between the energy flux and the different strain and rotation tensors has indicated that: (i) while results give some support to Smagorinski-like closure, at variance with pure hydrodynamic turbulence MHD energy flux cannot be globally recovered with a simple formula and several eddy viscosities should be used; (ii) as pointed out in previous works, the vorticity tensor has little correlation and can be omitted from modelling, at least as

a first approximation; (iii) contrarily to what is commonly used, we have found that the magnetic strain tensor $S_{b,\ell}$ contribution is not negligible with respect to the anti-symmetric rotation $\Omega_{b,\ell}$ one, with regard to the entire flux, so both $S_{b,\ell}$ and $\Omega_{b,\ell}$ need to be used to model subscale stresses. Finally (iv) we have found that the presence of a large magnetic field has an impact on the local shape of the energy flux, and the flux in regions of very high magnetic field has reduced forward fluctuations.

Present results indicate new directions for optimizing subgrid scale models in MHD turbulent flows. Many open questions still remain that future research should address. In particular the correlation between the local energy flux Π_ℓ and physically motivated combinations of the tensors $\Omega_{u,\ell}, \Omega_{b,\ell}, S_{u,\ell}, S_{b,\ell}$ would be a next step. Theoretical work in the same spirit as in the Clark model (Meneveau & Katz 2000) can also help in this direction. We plan to address these issues in our future work.

This work was granted access to the HPC resources of MesoPSL financed by the Région Ile de France and the project Equip@Meso (reference ANR-10-EQPX-29-01) of the programme Investissements d'Avenir supervised by the Agence Nationale pour la Recherche and the HPC resources of TGCC & CINES (allocations No. A0090506421 A0110506421 & No. A0062B10759) attributed by GENCI (Grand Equipement National de Calcul Intensif) where the present numerical simulations were performed. This work was also supported by the Agence nationale de la recherche (ANR DYSTURB project No. ANR-17-CE30-0004)

REFERENCES

Agullo, Olivier, Müller, W-C, Knaepen, Bernard & Carati, Daniele 2001 Large eddy simulation of decaying magnetohydrodynamic turbulence with dynamic subgrid-modeling. *Physics of Plasmas* **8** (7), 3502–3505.

Alexakis, Alexandros 2013 Large-scale magnetic fields in magnetohydrodynamic turbulence. *Physical Review Letters* **110** (8), 084502.

Alexakis, Alexandros & Biferale, Luca 2018 Cascades and transitions in turbulent flows. *Physics Reports* **767**, 1–101.

Alexakis, Alexandros & Chibbaro, Sergio 2020 Local energy flux of turbulent flows. *Physical Review Fluids* **5** (9), 094604.

Alexakis, Alexandros, Mininni, Pablo D & Pouquet, Annick 2005 Shell-to-shell energy transfer in magnetohydrodynamics. i. steady state turbulence. *Physical Review E* **72** (4), 046301.

Alexakis, A, Mininni, Pablo Daniel & Pouquet, A 2007 Turbulent cascades, transfer, and scale interactions in magnetohydrodynamics. *New Journal of Physics* **9** (8), 298.

Aluie, Hussein 2017 Coarse-grained incompressible magnetohydrodynamics: analyzing the turbulent cascades. *New Journal of Physics* **19** (2), 025008.

Aluie, Hussein & Eyink, Gregory L 2009 Localness of energy cascade in hydrodynamic turbulence. ii. sharp spectral filter. *Physics of Fluids* **21** (11), 115108.

Aluie, Hussein & Eyink, Gregory L 2010 Scale locality of magnetohydrodynamic turbulence. *Physical review letters* **104** (8), 081101.

Battaner, Eduardo 1996 *Astrophysical fluid dynamics*. Cambridge University Press.

Beresnyak, Andrey 2011 Spectral slope and kolmogorov constant of mhd turbulence. *Physical Review Letters* **106** (7), 075001.

Bian, Xin & Aluie, Hussein 2019 Decoupled cascades of kinetic and magnetic energy in magnetohydrodynamic turbulence. *Physical review letters* **122** (13), 135101.

Bian, Xin, Shang, Jessica K, Blackman, Eric G, Collins, Gilbert W & Aluie, Hussein 2021 Scaling of turbulent viscosity and resistivity: Extracting a scale-dependent turbulent magnetic prandtl number. *The Astrophysical Journal Letters* **917** (1), L3.

Biferale, Luca, Bonaccorso, Fabio, Buzzicotti, Michele & Iyer, Kartik P 2019 Self-

similar subgrid-scale models for inertial range turbulence and accurate measurements of intermittency. *Physical review letters* **123** (1), 014503.

Biskamp, Dieter 2003 *Magnetohydrodynamic turbulence*. Cambridge University Press.

Boldyrev, Stanislav 2006 Spectrum of magnetohydrodynamic turbulence. *Phys. Rev. Lett.* **96**, 115002.

Borue, Vadim & Orszag, Steven A 1998 Local energy flux and subgrid-scale statistics in three-dimensional turbulence. *Journal of Fluid Mechanics* **366**, 1–31.

Brandenburg, Axel, Sokoloff, Dmitry & Subramanian, Kandaswamy 2012 Current status of turbulent dynamo theory. *Space Science Reviews* **169** (1), 123–157.

Brandenburg, Axel & Subramanian, Kandaswamy 2005 Astrophysical magnetic fields and nonlinear dynamo theory. *Physics Reports* **417** (1-4), 1–209.

Bruno, Roberto & Carbone, Vincenzo 2013 The solar wind as a turbulence laboratory. *Living Reviews in Solar Physics* **10** (1), 1–208.

Buzzicotti, M, Linkmann, M, Aluie, H, Biferale, L, Brasseur, J & Meneveau, C 2018 Effect of filter type on the statistics of energy transfer between resolved and subfilter scales from a-priori analysis of direct numerical simulations of isotropic turbulence. *Journal of Turbulence* **19** (2), 167–197.

Camporeale, Enrico, Sorriso-Valvo, Luca, Califano, Francesco & Retinò, Alessandro 2018 Coherent structures and spectral energy transfer in turbulent plasma: a space-filter approach. *Physical review letters* **120** (12), 125101.

Carrasco, Federico, Viganò, Daniele & Palenzuela, Carlos 2020 Gradient subgrid-scale model for relativistic mhd large-eddy simulations. *Physical Review D* **101** (6), 063003.

Casciola, CM, Gualtieri, P, Benzi, R & Piva, R 2003 Scale-by-scale budget and similarity laws for shear turbulence. *Journal of Fluid Mechanics* **476**, 105–114.

Cerri, SS & Camporeale, E 2020 Space-filter techniques for quasi-neutral hybrid-kinetic models. *Physics of Plasmas* **27** (8), 082102.

Chen, Qiaoning, Chen, Shiyi & Eyink, Gregory L 2003 The joint cascade of energy and helicity in three-dimensional turbulence. *Physics of Fluids* **15** (2), 361–374.

Chen, Shiyi, Eyink, Gregory L, Wan, Minping & Xiao, Zuoli 2006 Is the kelvin theorem valid for high reynolds number turbulence? *Physical review letters* **97** (14), 144505.

Chernyshov, Alexander Aleksandrovich, Karelsky, Kirill Vladimirovich & Petrosyan, Arakel Sarkisovich 2014 Subgrid-scale modeling for the study of compressible magnetohydrodynamic turbulence in space plasmas. *Physics-Uspekhi* **57** (5), 421.

Cimarelli, A, De Angelis, E & Casciola, CM 2013 Paths of energy in turbulent channel flows. *Journal of Fluid Mechanics* **715**, 436–451.

Danaila, L, Anselmet, F, Zhou, Tongming & Antonia, RA 2001 Turbulent energy scale budget equations in a fully developed channel flow. *Journal of Fluid Mechanics* **430**, 87–109.

Dar, Gaurav, Verma, Mahendra K & Eswaran, V 2001 Energy transfer in two-dimensional magnetohydrodynamic turbulence: formalism and numerical results. *Physica D: Nonlinear Phenomena* **157** (3), 207–225.

Davidson, Peter Alan 2002 *An introduction to magnetohydrodynamics*. Cambridge University Press.

Domaradzki, J Andrzej, Teaca, Bogdan & Carati, Daniele 2009 Locality properties of the energy flux in turbulence. *Physics of fluids* **21** (2), 025106.

Dubrulle, Bérengère 2019 Beyond kolmogorov cascades. *Journal of Fluid Mechanics* **867**.

Eyink, G & Sreenivasan, K 2006 Onsager and the theory of hydrodynamic turbulence. *Reviews of Modern Physics* .

Eyink, Gregory, Vishniac, Ethan, Lalescu, Cristian, Aluie, Hussein, Kanov, Kalin, Bürger, Kai, Burns, Randal, Meneveau, Charles & Szalay, Alexander 2013 Flux-freezing breakdown in high-conductivity magnetohydrodynamic turbulence. *Nature* **497** (7450), 466–469.

Eyink, Gregory L 2005 Locality of turbulent cascades. *Physica D: Nonlinear Phenomena* **207** (1-2), 91–116.

Eyink, Gregory L 2018 Cascades and dissipative anomalies in nearly collisionless plasma turbulence. *Physical Review X* **8** (4), 041020.

Eyink, Gregory L & Aluie, Hussein 2009 Localness of energy cascade in hydrodynamic turbulence. i. smooth coarse graining. *Physics of Fluids* **21** (11), 115107.

Frisch, U. 1995 *Turbulence. The legacy of A.N Kolmogorov*. Cambridge, University press.

Galtier, S 2009 Exact vectorial law for axisymmetric magnetohydrodynamics turbulence. *The Astrophysical Journal* **704** (2), 1371.

Galtier, Sébastien 2016 *Introduction to modern magnetohydrodynamics*. Cambridge University Press.

Galtier, Sébastien 2018 On the origin of the energy dissipation anomaly in (hall) magnetohydrodynamics. *Journal of Physics A: Mathematical and Theoretical* **51** (20), 205501.

Germano, Massimo 1992 Turbulence: the filtering approach. *Journal of Fluid Mechanics* **238**, 325–336.

Germano, Massimo, Piomelli, Ugo, Moin, Parviz & Cabot, William H 1991 A dynamic subgrid-scale eddy viscosity model. *Physics of Fluids A: Fluid Dynamics* **3** (7), 1760–1765.

Goldreich, P & Sridhar, S 1995 Toward a theory of interstellar turbulence. 2: Strong alfvenic turbulence. *The Astrophysical Journal* **438**, 763–775.

Goldstein, Melvyn L, Roberts, D_ A & Matthaeus, WH 1995 Magnetohydrodynamic turbulence in the solar wind. *Annual review of astronomy and astrophysics* **33** (1), 283–325.

Grete, Philipp, Vlaykov, Dimitar G, Schmidt, Wolfram & Schleicher, Dominik RG 2017 Comparative statistics of selected subgrid-scale models in large-eddy simulations of decaying, supersonic magnetohydrodynamic turbulence. *Physical Review E* **95** (3), 033206.

Innocenti, Alessio, Jaccod, Alice, Popinet, Stéphane & Chibbaro, Sergio 2021 Direct numerical simulation of bubble-induced turbulence. *Journal of Fluid Mechanics* **918**.

Iroshnikov, PS 1964 Turbulence of a conducting fluid in a strong magnetic field. *Soviet Astronomy* **7**, 566.

Kessar, Mouloud, Balarac, Guillaume & Plunian, Franck 2016 The effect of subgrid-scale models on grid-scale/subgrid-scale energy transfers in large-eddy simulation of incompressible magnetohydrodynamic turbulence. *Physics of Plasmas* **23** (10), 102305.

Kolmogorov, Andrey Nikolaevich 1941 The local structure of turbulence in incompressible viscous fluid for very large reynolds numbers. *Cr Acad. Sci. URSS* **30**, 301–305.

Kraichnan, Robert H 1965 Inertial-range spectrum of hydromagnetic turbulence. *The Physics of Fluids* **8** (7), 1385–1387.

Kraichnan, Robert H 1971 Inertial-range transfer in two-and three-dimensional turbulence. *Journal of Fluid Mechanics* **47** (3), 525–535.

Landau, Lev Davidovich, Bell, JS, Kearsley, MJ, Pitaevskii, LP, Lifshitz, EM & Sykes, JB 2013 *Electrodynamics of continuous media*, , vol. 8. elsevier.

Leonard, Athony 1975 Energy cascade in large-eddy simulations of turbulent fluid flows. In *Advances in geophysics*, , vol. 18, pp. 237–248. Elsevier.

Lesieur, Marcel, Métais, Olivier, Comte, Pierre & others 2005 *Large-eddy simulations of turbulence*. Cambridge university press.

Linkmann, Moritz, Buzzicotti, Michele & Biferale, Luca 2018 Multi-scale properties of large eddy simulations: correlations between resolved-scale velocity-field increments and subgrid-scale quantities. *Journal of Turbulence* **19** (6), 493–527.

Liu, Shewen, Meneveau, Charles & Katz, Joseph 1994 On the properties of similarity subgrid-scale models as deduced from measurements in a turbulent jet. *Journal of Fluid Mechanics* **275**, 83–119.

McKee, Christopher F & Ostriker, Eve C 2007 Theory of star formation. *Annu. Rev. Astron. Astrophys.* **45**, 565–687.

Meneveau, Charles 1994 Statistics of turbulence subgrid-scale stresses: Necessary conditions and experimental tests. *Physics of Fluids* **6** (2), 815–833.

Meneveau, Charles & Katz, Joseph 2000 Scale-invariance and turbulence models for large-eddy simulation. *Annual Review of Fluid Mechanics* **32** (1), 1–32.

Miesch, Mark, Matthaeus, William, Brandenburg, Axel, Petrosyan, Arakel, Pouquet, Annick, Cambon, Claude, Jenko, Frank, Uzdensky, Dmitri, Stone,

James, Tobias, Steve & others 2015 Large-eddy simulations of magnetohydrodynamic turbulence in heliophysics and astrophysics. *Space Science Reviews* **194** (1), 97–137.

Mininni, Pablo, Alexakis, Alexandros & Pouquet, Annick 2005 Shell-to-shell energy transfer in magnetohydrodynamics. ii. kinematic dynamo. *Physical Review E* **72** (4), 046302.

Mininni, Pablo D, Rosenberg, Duane, Reddy, Raghu & Pouquet, Annick 2011 A hybrid mpi–openmp scheme for scalable parallel pseudospectral computations for fluid turbulence. *Parallel computing* **37** (6-7), 316–326.

Misra, Ashish & Pullin, Dale I 1997 A vortex-based subgrid stress model for large-eddy simulation. *Physics of Fluids* **9** (8), 2443–2454.

Moll, Rainer, Graham, J Pietarila, Pratt, J, Cameron, RH, Müller, W-C & Schüssler, M 2011 Universality of the small-scale dynamo mechanism. *The Astrophysical Journal* **736** (1), 36.

Monin, A. S. & Yaglom, A. M. 1975 *Statistical Fluid Mechanics*. MIT Press, Cambridge, Mass.

Müller, Wolf-Christian & Carati, Daniele 2002 Dynamic gradient-diffusion subgrid models for incompressible magnetohydrodynamic turbulence. *Physics of plasmas* **9** (3), 824–834.

Piomelli, Ugo, Cabot, William H, Moin, Parviz & Lee, Sangsan 1991 Subgrid-scale backscatter in turbulent and transitional flows. *Physics of Fluids A: Fluid Dynamics* **3** (7), 1766–1771.

Politano, H & Pouquet, A 1998 von kármán–howarth equation for magnetohydrodynamics and its consequences on third-order longitudinal structure and correlation functions. *Physical Review E* **57** (1), R21.

Ponty, Yannick, Mininni, Pablo D, Laval, Jean-Philipe, Alexakis, Alexandros, Baerenzung, Julien, Daviaud, François, Dubrulle, Bérengère, Pinton, Jean-François, Politano, Héléne & Pouquet, Annick 2008 Linear and non-linear features of the taylor–green dynamo. *Comptes Rendus Physique* **9** (7), 749–756.

Pope, S. B. 2000 *Turbulent Flows*. Cambridge University Press.

Sagaut, P. 2001 *Large eddy simulation for incompressible flows*, , vol. 20. Springer.

Schekochihin, Alexander A, Cowley, Steven C, Taylor, Samuel F, Maron, Jason L & McWilliams, James C 2004 Simulations of the small-scale turbulent dynamo. *The Astrophysical Journal* **612** (1), 276.

Smagorinsky, Joseph 1963 General circulation experiments with the primitive equations: I. the basic experiment. *Monthly weather review* **91** (3), 99–164.

Sorriso-Valvo, Luca, Marino, Raffaele, Carbone, Vincenzo, Noullez, A, Lepreti, F, Veltri, P, Bruno, Roberto, Bavassano, Bruno & Pietropaolo, Ermanno 2007 Observation of inertial energy cascade in interplanetary space plasma. *Physical review letters* **99** (11), 115001.

Speziale, Charles G 1985 Galilean invariance of subgrid-scale stress models in the large-eddy simulation of turbulence. *Journal of fluid mechanics* **156**, 55–62.

Teaca, Bogdan, Carati, Daniele & Andrzej Domaradzki, J 2011 On the locality of magnetohydrodynamic turbulence scale fluxes. *Physics of Plasmas* **18** (11), 112307.

Teaca, Bogdan, Gorbunov, Evgeny A, Told, Daniel, Navarro, Alejandro Bañón & Jenko, Frank 2021 Sub-grid-scale effects in magnetised plasma turbulence. *Journal of Plasma Physics* **87** (2).

Teaca, Bogdan, Verma, MK, Knaepen, Bernard & Carati, Daniele 2009 Energy transfer in anisotropic magnetohydrodynamic turbulence. *Physical Review E* **79** (4), 046312.

Tennekes, H. & Lumley, J. L. 1990 *A First Course in Turbulence*. The MIT Press, Cambridge, Massachusetts.

Theobald, Michael L, Fox, Peter A & Sofia, Sabatino 1994 A subgrid-scale resistivity for magnetohydrodynamics. *Physics of plasmas* **1** (9), 3016–3032.

Valori, Valentina, Innocenti, Alessio, Dubrulle, Bérengère & Chibbaro, Sergio 2020 Weak formulation and scaling properties of energy fluxes in three-dimensional numerical turbulent rayleigh–bénard convection. *Journal of Fluid Mechanics* **885**.

Verma, Mahendra K 2004 Statistical theory of magnetohydrodynamic turbulence: recent results. *Physics Reports* **401** (5-6), 229–380.

Verma, Mahendra K 2019 *Energy transfers in fluid flows: multiscale and spectral perspectives*. Cambridge University Press.

Verma, Mahendra K 2021 Variable energy flux in turbulence. *Journal of Physics A: Mathematical and Theoretical* .

Verma, Mahendra K & Kumar, Shishir 2004 Large-eddy simulations of fluid and magnetohydrodynamic turbulence using renormalized parameters. *Pramana* **63** (3), 553–561.

Viganò, Daniele, Aguilera-Miret, Ricard & Palenzuela, Carlos 2019 Extension of the subgrid-scale gradient model for compressible magnetohydrodynamics turbulent instabilities. *Physics of Fluids* **31** (10), 105102.

Vlaykov, Dimitar G, Grete, Philipp, Schmidt, Wolfram & Schleicher, Dominik RG 2016 A nonlinear structural subgrid-scale closure for compressible mhd. i. derivation and energy dissipation properties. *Physics of Plasmas* **23** (6), 062316.

Vreman, Bert, Geurts, Bernard & Kuerten, Hans 1994 Realizability conditions for the turbulent stress tensor in large-eddy simulation. *Journal of Fluid Mechanics* **278**, 351–362.

Vreman, Bert, Geurts, Bernard & Kuerten, Hans 1997 Large-eddy simulation of the turbulent mixing layer. *Journal of fluid mechanics* **339**, 357–390.

Yang, Yan, Matthaeus, William H, Roy, Sohom, Roytershteyn, Vadim, Parashar, Tulasi N, Bandyopadhyay, Riddhi & Wan, Minping 2022 Pressure–strain interaction as the energy dissipation estimate in collisionless plasma. *The Astrophysical Journal* **929** (2), 142.